Hindawi Publishing Corporation
International Journal of Navigation and Observation
Volume 2008, Article ID 246703, 14 pages
doi:10.1155/2008/246703

Research Article

Design of Short Synchronization Codes for Use in Future GNSS System

Surendran K. Shanmugam,[1] Cécile Mongrédien,[1] John Nielsen,[2] and Gérard Lachapelle[1]

[1] *Department of Geomatics Engineering, University of Calgary, AB, Canada T2N 1N4*
[2] *Department of Electrical and Computer Engineering, University of Calgary, AB, Canada T2N 1N4*

Correspondence should be addressed to Surendran K. Shanmugam, suren@geomatics.ucalgary.ca

Received 4 August 2007; Accepted 7 February 2008

Recommended by Olivier Julien

The prolific growth in civilian GNSS market initiated the modernization of GPS and the GLONASS systems in addition to the potential deployment of Galileo and Compass GNSS system. The modernization efforts include numerous signal structure innovations to ensure better performances over legacy GNSS system. The adoption of secondary short synchronization codes is one among these innovations that play an important role in spectral separation, bit synchronization, and narrowband interference protection. In this paper, we present a short synchronization code design based on the optimization of judiciously selected performance criteria. The new synchronization codes were obtained for lengths up to 30 bits through exhaustive search and are characterized by optimal periodic correlation. More importantly, the presence of better synchronization codes over standardized GPS and Galileo codes corroborates the benefits and the need for short synchronization code design.

1. INTRODUCTION

The legacy global positioning system (GPS) has performed well beyond initial expectations in the past but faces stern impediments in the view point of new civilian GPS applications. Several initiatives were launched during the last decade to satisfy the demands of these new civilian applications. Consequently, these efforts led to the birth of second-generation global navigation satellite systems (GNSSs). These efforts include the modernization of legacy GPS and the restoration of Russian global navigation satellite system (GLONASS). The Galileo system, a major European initiative, is well positioned to benefit from the three decades of GPS and GLONASS experience [1]. More recently, the GNSS community has witnessed yet another highpoint with the launch of first medium earth orbit (MEO) satellite of Chinese Compass GNSS system [2].

A major milestone in the modernization initiative is the inclusion of new civilian signals that will provide the benefits of frequency diversity besides accuracy and availability improvements [3–5]. These new civilian signals include numerous structural innovations that will provide the foremost benefit to the civilian GNSS community. The modernized signals encompass key innovations such as dataless channel, improved navigation data message format, secondary spreading code structure, and new modulations schemes [6]. More specifically, both GPS and Galileo systems utilize secondary short synchronization codes to accomplish

(i) data symbol synchronization,

(ii) spectral separation,

(iii) narrowband interference protection.

For instance, the use of short 10-bit and 20-bit Neuman-Hofman (NH) codes, in GPS L5 signals, readily alleviates the issue of data symbol synchronization. Besides, the different code period of NH10 and NH20 codes in the data and pilot channels readily provides the necessary spectral separation. The secondary synchronization code further enhances the correlation suppression performance of the primary pseudorandom noise (PRN) code. Finally, it spreads the spectral lines of primary PRN I5/Q5 codes thereby reducing the effect of narrowband interference by another 13 dB [4]. The Galileo system also utilizes short secondary synchronization codes of various lengths to facilitate the aforementioned tasks [7].

Table 1: Secondary code assignment in GPS and Galileo systems.

GPS			Galileo		
Signal type	Code name	Code length	Signal type	code name	Code length
L5-Data	NH10	10	E5a-Data	CS20	20
L5-Pilot	NH20	20	E5a-Pilot	$CS100_{1-50}$	100
L1C-Pilot	$OC1800_{1-210}$	1800	E1c	CS25	25
			E5b-Data	CS4	4
			E5b-Pilot	$CS100_{51-1001}$	100
			E6c	$CS100_{1-50}$	100

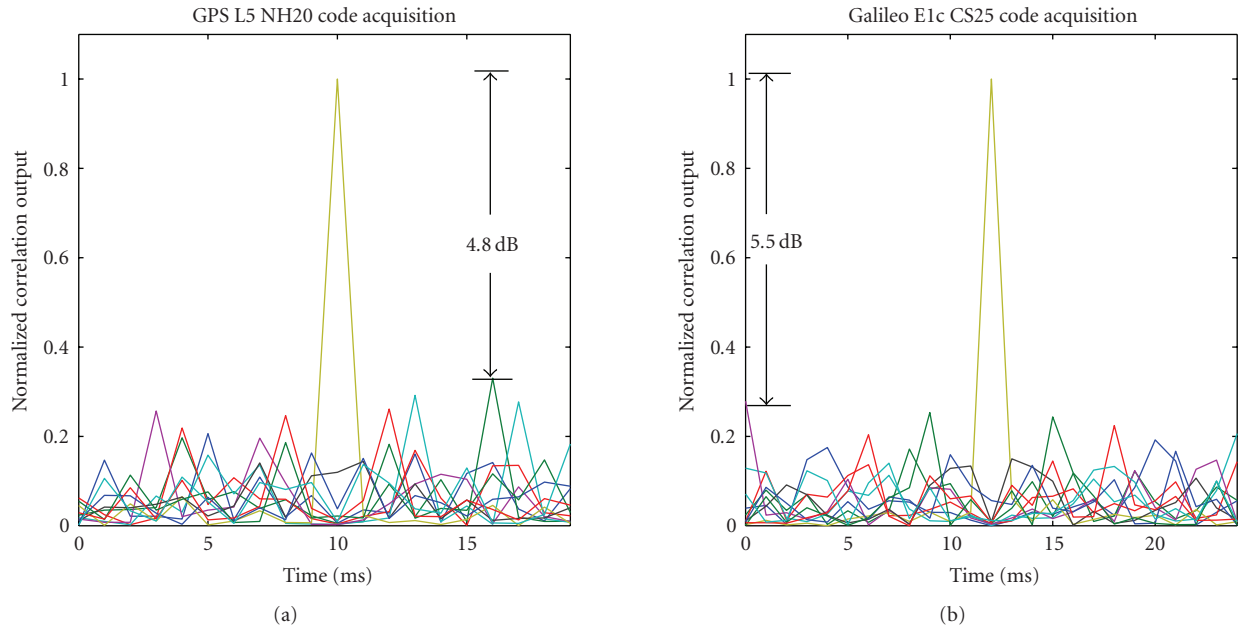

Figure 1: Superposition of secondary code correlation outputs for various Doppler offsets. (LHS) GPS L5 NH20 code (RHS) Galileo E1c CS25 code.

Table 1 lists the secondary code assignments and their lengths in GPS and Galileo systems.

The secondary synchronization codes are predominantly memory codes except for the L1C, wherein the overlay codes were obtained through truncated *m*-sequences (1–63) and gold sequences (64–210) [8]. There exists a trade-off between memory codes and codes that are obtained from linear feedback shift register (LFSR) implementation. While the LFSR-based codes are appealing in the view point of hardware implementation, they only exist for specific lengths. The use of truncation technique can alleviate this issue at the expense of inferior correlation properties. On the other hand, memory codes can be obtained for any specific lengths with optimal correlation characteristics. However, exhaustive search of optimal synchronization code becomes more difficult with increasing code lengths.

A limitation arising due to the usage of short synchronization codes is the degradation in correlation suppression especially in the presence of frequency errors. For instance, the vulnerability of NH20 code acquisition in the presence of Doppler uncertainties is discussed in [9]. The isolation of the main correlation peak to that of secondary peaks can degrade from the nominal 14 dB to 4.8 dB level under worst case Doppler scenarios [10]. Under these conditions, the NH code acquisition of weak GPS L5 signals becomes more difficult in the presence of other strong GPS L5 signals. The existence of better synchronization codes over standardized NH20 code was later reported in [10], which is based on the 20-bit synchronization code originally proposed in [11]. Under specific Doppler conditions, the new 20-bit code (known as the Merten's code) showed an improvement of around 2 dB over the standardized NH20 code in terms of correlation suppression [10]. However, the performance improvement achieved by the Merten's code corresponds to a specific Doppler scenario and thus does not reflect the actual performance improvement under Doppler uncertainty. Interestingly, the importance of spreading code selection for the Galileo GNSS system and the corresponding measures was identified in [12]. Besides, it is also desirable to develop optimal synchronization codes that offer better

resistance to residual Doppler errors. In this paper, we introduce relative performance measures such as peak-to-side lobe ratio (PSLR) and integrated side lobe ratio (ISLR) related to the design of periodic binary codes that are utilized in GNSS system. More importantly, new optimal secondary synchronization codes were obtained using these performance measures through exhaustive search for lengths up to 30 bits. The merits of the proposed synchronization codes are also compared with standardized codes using the same performance measures. Besides, the association of the optimal synchronization codes with the systematic codes such as Golay complementary codes is also established. Numerical simulations were used to demonstrate the superior acquisition performance of the proposed short synchronization codes over standardized codes under Doppler uncertainties in terms of PSLR measure.

The remainder of this paper is organized as follows. In Section 2, the advantage of optimal synchronization codes is further established in the view point of GPS L5 NH code acquisition. More specifically, we show the inadequacy of NH20 code in comparison to Merten's 20-bit code under different Doppler conditions. The relevant performance measures pertaining to optimal binary periodic synchronization code are introduced in Section 3. The binary-code search strategy and the various code construction methods are detailed in Section 4. Besides, the merits of new synchronization codes are compared with the standardized codes. Acquisition performance analysis is then carried out in Section 5. The final concluding remarks are made in Section 6.

2. NEED FOR IMPROVED SYNCHRONIZATION CODES

An issue with short synchronization codes is limited correlation suppression performance due to their short code length. For instance, the correlation suppression performance of NH20 code can be degraded by as much as 8 dB from the nominal 14 dB in the presence of Doppler uncertainty [9]. In [10], the authors reported a degradation of 9.2 dB for NH20 code under specific Doppler scenarios. To further illustrate this, the GPS L5 NH20 code and Galileo E1c CS25 code correlation outputs for different Doppler bins are plotted in Figure 1. The acquisition criterion in Figure 1 was obtained following the analysis reported in [10]. For instance, the residual Doppler during the acquisition of NH20 and CS25 code was set to 12 Hz; and this residual Doppler was searched between 0 and 250 Hz in steps of 25 Hz.

In Figure 1, we can readily observe the degradation in correlation main peak isolation for NH20 from the nominal 14 dB to 4.8 dB as reported earlier in [10]. On the other hand, the Galileo E1c CS25 code degraded from the nominal 18.4 dB down to 5.5 dB. The additional 3 dB degradation in CS25 code acquisition can be attributed to the longer coherent integration time (i.e., 25 millie seconds rather than 20 millie seconds) and nonzero out-of-phase correlation in the original CS25 code. Accordingly, the acquisition of weak GPS L5 signals or Galileo E1c signals can be hindered in the presence of strong GPS L5 and Galileo E1c signals from other satellites. While the correlation suppression performance can be improved with longer length codes, judicial selection of synchronization codes can offer better correlation suppression for the same code length. For example, in [10], the authors reported a correlation suppression gain of around 2 dB for Merten's code over standard NH20 code under specific Doppler scenario. The LHS plot in Figure 2 shows the superposition of the Merten's 20-bit synchronization code (M20) correlation outputs for the same Doppler setting as in Figure 1. The RHS plot shows the correlation suppression performance for the standardized NH20 and the M20 code for various residual Doppler's. The Doppler was searched between 0 to 250 Hz in steps of 25 Hz.

The RHS plot in Figure 2 readily shows the 2 dB improvement accomplished by the M20 code over the standardized NH20 code for the residual Doppler of 12 Hz. In other words, the M20 code can tolerate another 10 Hz of residual Doppler for the same PSLR of 4.8 dB achieved by the NH20 code. The M20 code resulted in an average performance improvement of around 1.7 dB over the NH20 code for the range of residual Doppler's. The performance improvement in M20 code can readily be accredited to its better correlation characteristic. For instance, the periodic correlation of the different synchronization codes of length 20 (see Table 2) is summarized below

$$\begin{aligned}
R_{\mathrm{NH10}} &= \{10,-2,2,-2,-2,2,-2,-2,2,-2\},\\
R_{\mathrm{NH20}} &= \{20,0,0,0,0,0,-4,0,4,0,-4,0,4,0,-4,0,0,0,0,0\},\\
R_{\mathrm{CS20}} &= \{20,0,0,0,0,0,4,0,-4,0,-4,0,-4,0,4,0,0,0,0,0\},\\
R_{\mathrm{M20}} &= \{20,0,0,0,0,-4,0,-4,0,0,0,0,0,-4,0,-4,0,0,0,0\}.
\end{aligned} \tag{1}$$

The periodic correlation output of the M20 code, R_{M20}, has lesser number of out-of-phase correlation when compared to both NH20 and CS20 codes. Accordingly, one can expect its code acquisition performance to be superior even in the presence of residual Doppler. It is worth emphasizing here that the NH10 and NH20 codes were not obtained from exhaustive search, whereas the M20 code was obtained through exhaustive search [11]. The very existence of the NH20, M20, and CS20 corroborates the presence of multiple solutions for the code design problem. Besides, the search for periodic code is expected to yield multiple solutions due to the existence of equivalence classes [13]. Hence, it is necessary to obtain the binary codes that satisfy the optimal correlation characteristics and select the best possible code judiciously using relevant performance measures.

3. OPTIMAL SYNCHRONIZATION CODE—FIGURE OF MERITS

Better synchronization code can be obtained by optimizing the corresponding correlation characteristics of the individual codes. As we are dealing with binary codes of short period, the optimization of correlation characteristics can be achieved in an exhaustive fashion. It is however, necessary to derive performance measure or measures that readily embody the correlation characteristics of a binary code [12]. The two important performance measures pertaining

Table 2: Optimal binary synchronization code search result.

Code length	Number of codes	PSLR (dB)	ISLR (dB)	Code length	Number of codes	PSLR (dB)	ISLR (dB)
4	**8 (1)**	**∞**	**∞**	18	6,047 (168)	19.1	2.4
5	10 (1)	14	3.2	19	75 (2)	22.6	10
6	47 (8)	9.5	0.9	**20**	**5,079 (45)**	**14**	**3.1**
7	28 (2)	16.9	4.1	21	1,259 (30)	16.9	4.2
8	32 (2)	6	2	22	15,839 (360)	20.8	2.9
9	108 (8)	9.5	1.7	23	91 (2)	27.3	12
10	**360 (16)**	**14**	**1.4**	24	1,535 (32)	15.6	9
11	44 (4)	20.8	6.1	**25**	**7,000 (260)**	**18.4**	**4.3**
12	96 (4)	9.5	4.5	26	31,615 (608)	22.3	3.4
13	104 (4)	22.3	7.1	27	775 (144)	19.1	4.9
14	1,791 (128)	16.9	1.9	28	23,743 (424)	16.9	4.1
15	59 (4)	23.5	8	29	3,247 (56)	19.7	4.6
16	255 (16)	12	2.7	30	35,039 (584)	23.5	3.9
17	2,175 (64)	15.1	2.3				

to optimal synchronization codes are the peak-to-side lobe ratio (PSLR) [14] and the integrated side lobe ratio (ISLR) [15]. Besides, the synchronization codes are also expected to be *balanced* for desirable spectral characteristics. To define PSLR and ISLR, we first express the periodic auto-correlation of the binary code of length N (i.e., $\mathbf{x} = [x_0, x_1, \ldots, x_{N-1}]$), at shift i, as

$$R(i) = \sum_{k=0}^{N-1} x(k)x(k - i \bmod N), \quad i = 0, 1, 2, \ldots, N-1, \tag{2}$$

where $x(k) \in \{+1, -1\}$ and **mod** is the modulo operation. The PSLR for the binary code $x(k)$ with the periodic auto-correlation, $R(i)$, is given by

$$\mathrm{PSLR}(\mathbf{x}) = \frac{R(i=0)^2}{\max |R(i \neq 0)|^2}, \quad i = 0, 1, 2, \ldots, N-1. \tag{3}$$

Maximizing the PSLR measure minimizes the out-of-phase correlation that eventually aids in reducing false acquisition. On the other side, ISLR measures the ratio of auto-correlation main lobe (or peak) energy to its side lobe energy [15]. The ISLR of a binary code is defined as

$$\mathrm{ISLR}(\mathbf{x}) = \frac{N^2}{2\sum_{i=1}^{N-1} |R(i)|^2}, \quad i = 0, 1, 2, \ldots, N-1. \tag{4}$$

Maximizing the ISLR measure readily limits the effect of out-of-phase correlation from all shifts. It will be emphasized here that the maximization of ISLR often maximizes the PSLR measure. Finally, the balanced property of a binary code is related to the mean value of the code and is given by

$$\mu(\mathbf{x}) = \frac{1}{N} \sum_{k=0}^{N-1} x(k). \tag{5}$$

For binary code sets design, as in the case of OC1800 in GPS and CS100 in Galileo, it is also desirable to minimize the mutual interference experienced by the individual codes from other codes. Minimizing the magnitude of cross-correlation readily limits the effect of mutual interference between any two codes. The *mean square correlation* (MSC) measure embodies this mutual correlation and can be utilized during multiobjective synchronization code optimization. For any two codes $x_p(k)$ and $x_q(k)$ of length N pertaining to the code set comprising of M unique codes, the mutual correlation or the MSC is given by

$$\mathrm{MSC}(p, q) = 2 \sum_{i=0}^{N-1} |R_{p,q}(i)|^2, \quad p \neq q, \tag{6}$$

where $R_{p,q}(i)$ is the periodic cross-correlation between the codes $x_p(k)$ and $x_q(k)$, and is given by

$$R_{p,q}(i) = \sum_{k=0}^{N-1} x_p(k)x_q(k - i \bmod N), \quad i = 0, 1, 2, \ldots, N-1. \tag{7}$$

The aforementioned mean square correlation is closely related to the well-known total squared correlation measure utilized in CDMA spread code optimization [16].

4. OPTIMUM CODE SEARCH RESULTS

For short code length, the synchronization code optimization can be accomplished through exhaustive search of binary codes with optimal correlation characteristics. The developed exhaustive search technique utilized fast Fourier transform (FFT)-based block processing and matrix manipulations to speed up the search process. Both PSLR and ISLR were utilized for the objective maximization. Optimal synchronization codes for lengths up to 30 were obtained through exhaustive search. Interestingly, the search process yielded large number of codes that were optimal based on the aforementioned performance measures. Table 2 lists the number of codes alongside the unique solutions within braces, the PSLR and ISLR values, respectively.

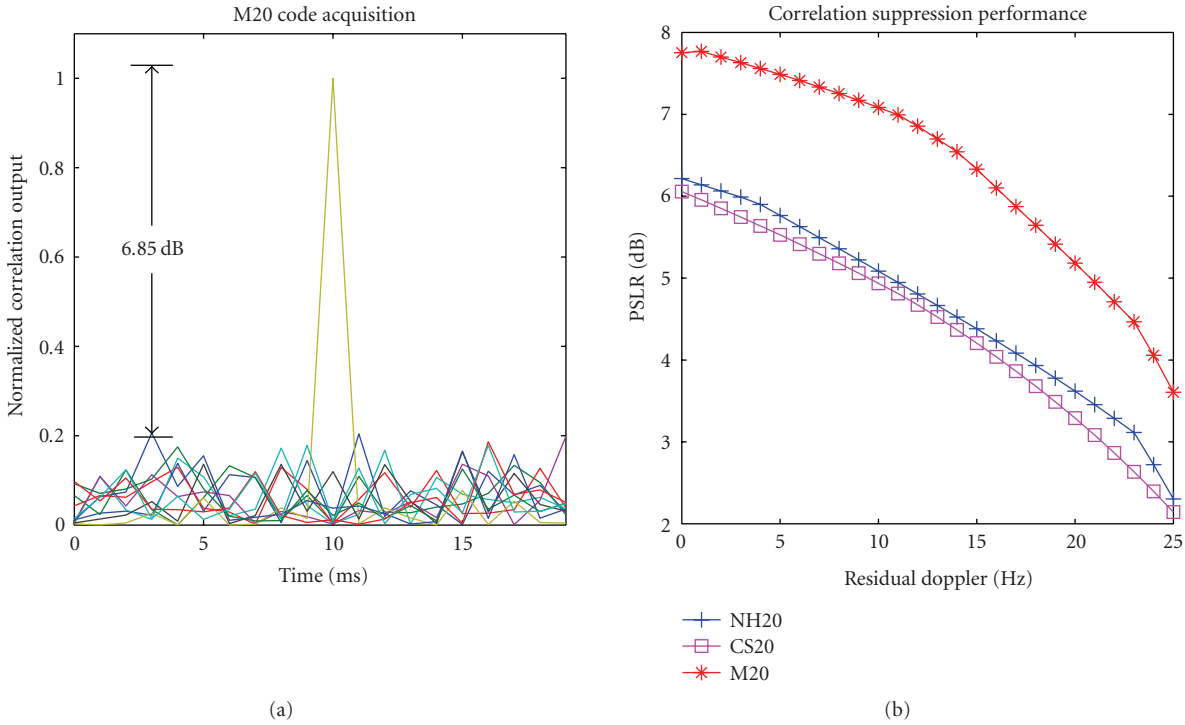

FIGURE 2: (LHS) superposition of secondary code correlation outputs for various Doppler offsets for M20 code (RHS) PSLR performance as a function of residual Doppler.

The large number of codes arise from existence of the equivalence classes due to the shift invariance property of the periodic codes [13]. For example, the code $x(k)$, its negated version, its time reversed, or its shifted version will be characterized by similar PSLR and ISLR measures. To obtain unique solutions, the search technique discarded codes if their maximum cross-correlation is equal to the code length. Accordingly, any two codes $x_p(k)$ and $x_q(k)$ satisfy the following cross-correlation constraint are considered unique:

$$\mathbf{max}\left|R_{p,q}(i)\right| < N, \quad i = 0, 1, 2, \ldots, N-1. \tag{8}$$

Besides, the codes are time-reversed and hence were tested for (8). While the balance property (i.e., $\mu(\mathbf{x})$) was not included during the code selection, its significance will be emphasized during the acquisition performance analysis. In Table 2, the binary codes whose lengths are similar to the standardized codes are highlighted in bold. In [17], the authors theoretically established the optimal periodic correlation of a *balanced* binary code as

$$R(i) = \begin{cases} 0 \text{ or } -4 & N \textbf{ mod } 4 = 0, \\ 2 \text{ or } -2 & N \textbf{ mod } 4 = 2, \end{cases} \quad i \neq 0. \tag{9}$$

The periodic correlation of optimal binary code for both odd and even lengths was further established in [18], and is expressed below

$$R(i) = \begin{cases} 0 \text{ or } 4 \text{ or } -4 & N \textbf{ mod } 4 = 0, \\ 1 \text{ or } -3 & N \textbf{ mod } 4 = 1, \\ 2 \text{ or } -2 & N \textbf{ mod } 4 = 2, \\ -1 \text{ or } 3 & N \textbf{ mod } 4 = 3, \end{cases} \quad i \neq 0. \tag{10}$$

From (1) and (9), we see that both NH10 and M20 possess optimal periodic correlation. Besides, the Galileo CS25 code was also optimal as it satisfied the periodic correlation expressed in (10). On the other hand, both NH20 and CS20 are not optimal in the view point of (9), but can be considered optimal in terms of PSLR measure. The inferior periodic correlation of NH20 does not come as a surprise as the original NH codes were not obtained by exhaustive search [19]. It should be noted here that all the secondary codes utilized in GPS and Galileo system are not balanced (i.e., sum of individual code phases is not equal to zero) and thus (9) cannot be applied in a strict sense, but indicates the conditions for optimality. Numerical analysis later confirmed the fact that even unbalanced binary code is characterized by periodic correlation as predicted in (9).

All the binary codes obtained through exhaustive search indeed satisfied the periodic correlation as expressed in (10) and thereby asserting the optimality of the developed binary codes. The optimal 10-bit and 25-bit code obtained through exhaustive search resulted in similar PSLR and ISLR performance measures to that of NH10 and CS25 codes in accordance to (10). On the other hand, the 20-bit code obtained via exhaustive search resulted in better

ISLR performance even as the PSLR performance was the same. Moreover, the new 20-bit code had similar correlation characteristics as that of M20 code introduced earlier. In Table 2, we can also observe that odd-length codes generally yielded better PSLR and ISLR performance. More specifically, the binary codes for lengths $N = 5, 7, 11, 13, 15$ showed similar PSLR and better ISLR, even when compared to twice their code lengths (i.e., $N = 10, 14, 22, 26, 30$). The high PSLR and ISLR values observed for code lengths $N = 5, 7, 11, 13, 15, 23$ can readily be attributed to their ideal correlation characteristics as expressed in (10). However, it is recognized that the choice of secondary code length in GNSS system can be influenced by other parameters besides correlation characteristics alone.

Further analysis of the optimal binary code of length 20 revealed the existence of close association of optimal binary codes to that of the well-known Golay complementary pairs [20]. The Golay complementary pairs have been extensively utilized in a number of applications ranging from radar signal processing [21] and communication [22] to multislit spectrometry [20]. Two binary codes $x_a(k)$ and $x_b(k)$ are said to be Golay complementary pair, if they satisfy the following constraint:

$$R_G(i) = R_a(i) + R_b(i) = \begin{cases} 2N, & i = 0, \\ 0, & i \neq 0, \end{cases} \tag{11}$$

where $R_a(i)$ and $R_b(i)$ are the periodic correlation of $x_a(k)$ and $x_b(k)$, respectively. $R_G(i)$ is the periodic correlation function of the Golay complementary pair. Besides, the individual codes in a Golay complementary pair are referred as Golay codes. The periodic correlation in (11) immediately asserts the advantage of Golay complementary codes in the view point of code design. For example, the NH10 code and the first-half of the NH20 code are Golay complementary pair as shown in Figure 3. Hence, there exists a possibility of utilizing this underlying structure to accomplish better acquisition abilities. Unfortunately, the NH10 code and second half of NH20 code are not Golay complementary pairs.

Motivated by this observation, the optimal binary codes of length 20 obtained via exhaustive search were tested for Golay complementary pair. Interestingly, many binary codes of length 20 obtained through exhaustive search (i.e., $S20_2$ in Table 3) satisfied the Golay complementary condition. For example, the Golay complementary pairs $G10_a$ and $G10_b$ can be constructed from the even and odd samples of $S20_2$ (hex value "05D39" and "FA2C6" also give rise to Golay pairs) listed in Table 3, and the corresponding Golay codes are given by

$$\begin{aligned} G10_a &= [-1, 1, -1, 1, -1, -1, -1, -1, 1, 1], \\ G10_b &= [1, -1, -1, 1, 1, -1, 1, 1, 1, 1]. \end{aligned} \tag{12}$$

More importantly, the individual Golay codes $G10_a$ and $G10_b$ were also optimal having periodic correlation in accordance to (9). Moreover, the Golay codes of length $N/2$ obtained from an optimal code of length N were also optimal. Consequently, the 45 optimal binary codes of length 20 (see Table 2) were tested for Golay complementary condition. Surprisingly, 75% (32 out of 45 codes) of the 20-bit optimal binary codes satisfied the Golay complementary condition. A corollary of this conjecture indicates the possibility of constructing optimal codes of length N from Golay complementary pairs of length $N/2$. The construction of binary codes by multiplexing Golay complementary pairs readily guarantees that every alternate shift will result in zero correlation due to the complementary correlation output of individual Golay codes. Interestingly, the aforementioned property of the Golay codes was utilized for signal acquisition in ultrasonic operations [23]. To further verify this corollary, we constructed a binary code from Golay complementary pairs of length 20 (hex values "CD87F" and "CE5AA"). The resulting binary code of length 40 (hex value "F0F6916EEE") demonstrated optimal periodic correlation as predicted by (9). Thus, it is possible to construct optimal binary codes of larger lengths by utilizing the aforementioned association between optimal codes and the Golay complementary codes. Besides, the highly regular structure of binary Golay complementary codes readily allows for an efficient construction [24].

Motivated by the aforementioned observation, we constructed synchronization codes of length $N = 100$ from optimal codes of lengths 10, 20, and 25. The specific choice of code length was dictated by the fact that the desired code length 100 was divisible by 10, 20, and 25. The final code length of 100 was obtained by manipulating the individual codes of length 10, 20, and 25 with the augmentation codes of length 10, 5 and 4. Let $x_p(k)$ and $x_s(k)$ be the primary and the augmentation code of length N_p and N_s. Thus, we have $N = N_s N_p$, where $N = 100$, $N_s = \{10, 5, 4\}$, and $N_p = \{10, 20, 25\}$ in our case. The final binary code, $x(k)$, of length N can be obtained as follows:

$$x(k) = \sum_{m=0}^{N_s-1} \sum_{n=0}^{N_p-1} x_s(m) x_p(n) g\left(k - m\frac{N}{N_s} - n\frac{N}{N_p}\right), \quad k = 0, 1, 2, \ldots, N-1, \tag{13}$$

where $g(k)$ is the rectangular pulse function and is given by

$$g(k + \Delta T) = \begin{cases} 1 & 0 \leq \Delta T < T_b, \\ 0 & \text{elsewhere}, \end{cases} \tag{14}$$

where T_b is the basic bit duration over which the x_k is constant. For example, the 100-bit code, $x(k)$ (hex value "C7F526E3FA9371FD49A7015B2"), was obtained from the primary code, $x_p(k)$ (hex value "380AD90"), and the augmentation code, $x_s(k)$ (hex value "1"). In Table 2, we saw that there exists 7,000 codes of length 25 with 260 unique solutions but we only need 100 unique codes. Thus, we utilized the following constraints on the PSLR and ISLR measures to limit the number of codes:

$$\begin{aligned} &\text{PSLR} \geq 21.9\ \text{dB}, \\ &\text{ISLR} \geq 3\ \text{dB}. \end{aligned} \tag{15}$$

The PSLR and ISLR thresholds in (15) were duly obtained from the average PSLR and ISLR measures of the Galileo

Table 3: Secondary synchronization code—performance measures ($\mu(\mathbf{x})$, PSLR, and ISLR are defined in (5), (3), and (4), resp.).

Secondary code performance									
Standard codes					Proposed codes				
Code identifier	Code length	$\lvert\mu(\mathbf{x})\rvert$	PSLR (dB)	ISLR (dB)	Code identifier	Code length	$\lvert\mu(\mathbf{x})\rvert$	PSLR (dB)	ISLR (dB)
CS4	4	0.5	∞	∞	S4	4	0.5	∞	∞
NH10	10	0.2	14	1.5	S10	10	0	14	1.5
NH20	20	0.2	14	4	$S20_1$	20	0	14	4
CS20	20	0.2	14	4	$S20_2$	20	0.1	14	4.9
CS25	25	0.2	18.4	6.3	$S20_3$	20	0.2	14	4
M4	4	0.5	∞	∞	$S25_1$	25	0.2	18.4	6.3
M10	10	0.4	14	1.5	$S25_2$	25	0.2	18.4	6.3
M20	20	0.1	14	4.9					
M25	25	0.2	18.4	6.3					

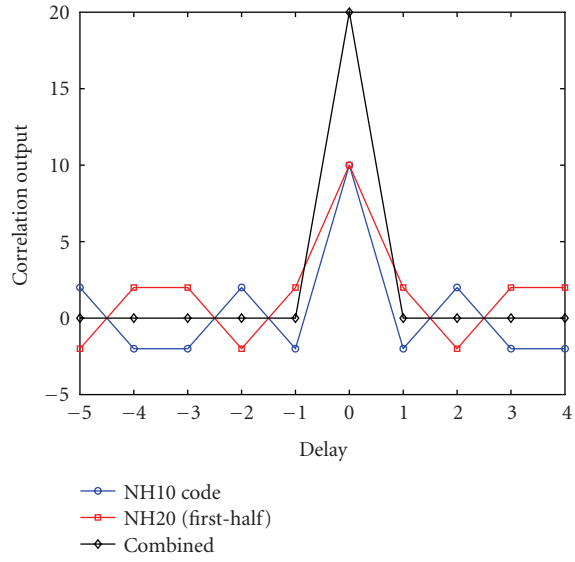

Figure 3: Correlation output of Golay complementary codes (NH10 and first half of NH20).

G100 code set [25]. Finally, the cross-correlation constraint expressed in (8) was also utilized to obtain unique solutions. Consequently, a total number of 105 unique codes were obtained in this fashion which satisfied the aforementioned conditions. The hexadecimal representations of the individual codes are listed in Table 6. It is worth noting here that not a single Galileo G100 code as well as the proposed 100-bit codes satisfied the optimal periodic correlation based on (9). The following section establishes the merits and limitations of the proposed binary synchronization codes in comparison to the standardized secondary synchronization codes.

5. ACQUISITION PERFORMANCE ANALYSIS

Having obtained the optimal binary codes of various lengths, we now turn our focus on the evaluation of the proposed codes in comparison to the standardized codes utilized in GPS and Galileo system. In this paper, the structure proposed in Tran and Hegarty [26] was adopted for the secondary code acquisition, wherein the primary code is assumed to be acquired within half chip duration alongside residual Doppler. The secondary code is acquired by correlating the primary code correlation outputs with the locally generated secondary code samples. The residual Doppler was assumed to be within ±250 Hz. During the secondary code acquisition, the residual Doppler was also searched within ±250 Hz in steps of 25 Hz.

The Galileo CS4 code is already established as the optimal code and will not be dealt during the acquisition performance analysis. Table 3 lists the $\mu(\mathbf{x})$, the PLSR, and the ISLR measures of the standardized Merten's and the proposed codes of various lengths. While the 20-bit synchronization codes achieved similar PSLR measure as that of 10-bit codes, their ISLR performances were much better than that of 10-bit codes. In Table 3, it can be noticed that there are 3 different sets of S20 code ($S20_1$, $S20_2$, and $S20_3$) and two sets of S25 code ($S25_1$ and $S25_2$). While these different codes are optimal in terms of correlation characteristics, their correlation characteristics differed in the presence of the residual Doppler with some outperforming the other codes. In Table 3, we see that the designed codes were not only optimal in terms of PSLR and ISLR measures, they were also more balanced. The advantage of the M20 and $S20_2$ over the NH20 and CS20 codes is readily asserted by the higher ISLR values. Interestingly, the other 20-bit codes $S20_1$ and $S20_3$ demonstrated better acquisition performance in comparison to M20 and $S20_2$ codes despite being inferior in ISLR measure. In the case of CS100 and S100 codes, the autocorrelation and cross-correlation protection were evaluated using a number of measures. The PSLR measure based on the auto-correlation was same for both CS100 and S100 codes despite being suboptimal in the view point of (9). The cross-correlation PSLR (CPSLR) measure was also obtained for CS100 and S100 codes. The CPSLR measures the ratio between the auto-correlation main peak of code ($R(i)$) to the maximum of the cross-correlation peak ($R_{p,q}(i)$) and it is given by

$$\text{CPSLR} = \frac{R(i=0)^2}{\mathbf{max}\left|R_{p,q}(i\neq 0)\right|^2}. \tag{16}$$

Table 4: Galileo CS100 and proposed S100 codes performance.

Secondary code performance						
	CPSLR (dB)		ISLR (dB)		MSC (dB)	
	CS100	S100	CS100	S100	CS100	S100
Max	14.9	14	6.6	5.9	43.5	43.6
Min	6	2.9	3.7	5.1	42.6	42.8
Mean	11.2	9.1	4.9	5.6	43	43.1
Std. Dev	1.2	2.4	0.6	0.3	0.1	0.2

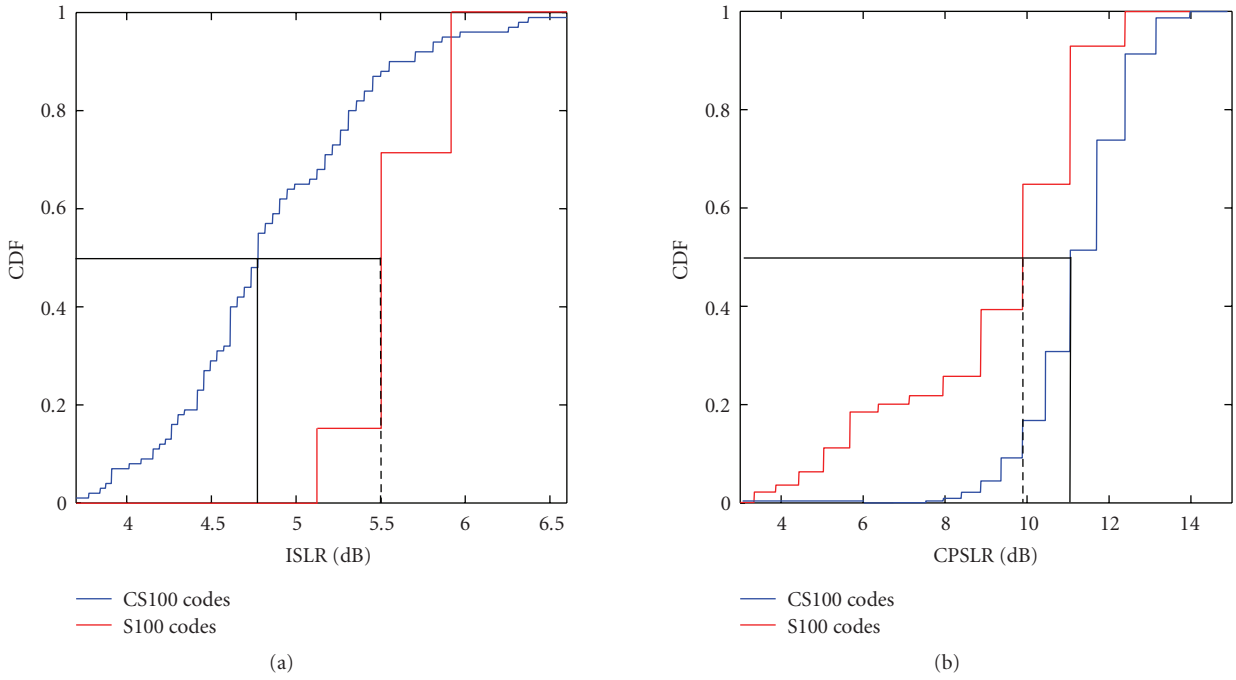

Figure 4: PSLR and ISLR performance of Galileo CS100 and the proposed S100 codes.

Table 5: Hexadecimal representation GPS/Galileo and proposed secondary codes (highlighted colour in bold represents equivalence).

Code identifier	Code length	Number of hex symbols	Number of zero padding	Hex value
CS4	4	1	0	**E**
NH10	10	3	2	F28
NH20	20	5	0	FB2B1
CS20	20	5	0	842E9
CS25	25	7	3	**380AD90**
M4	4	1	0	**D**
M10	10	3	2	CBC
M20	20	5	0	**FA2C6**
M25	25	7	3	**E3FA930**
S4	4	1	0	**B**
S10	10	3	2	3B0, 3C8
$S20_1$	20	5	0	14B37, 14B37
$S20_2$	20	5	0	**05D39**, 6345F
$S20_3$	20	5	0	315B0, 640E5
$S25_1$	25	7	3	21228F8, DFB45C0
$S25_2$	25	7	3	AD04C18

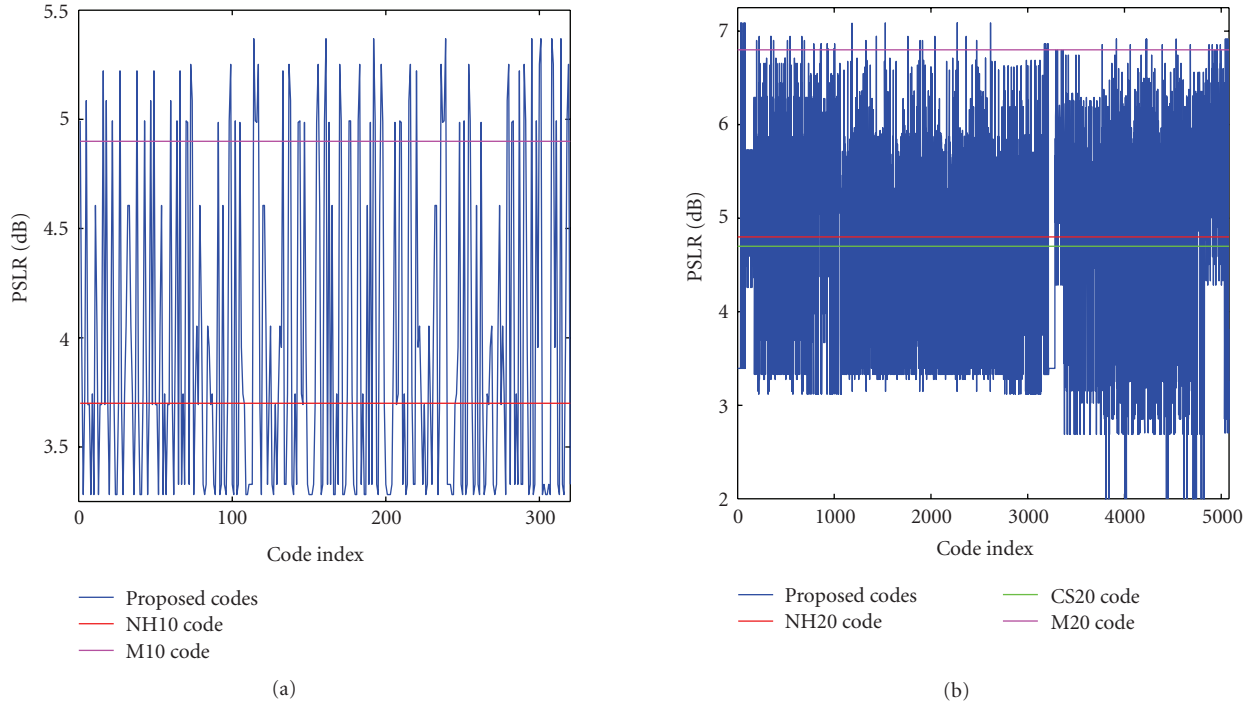

Figure 5: PSLR performance in the presence of residual Doppler (LHS) 10-bit code (RHS) 20-bit code.

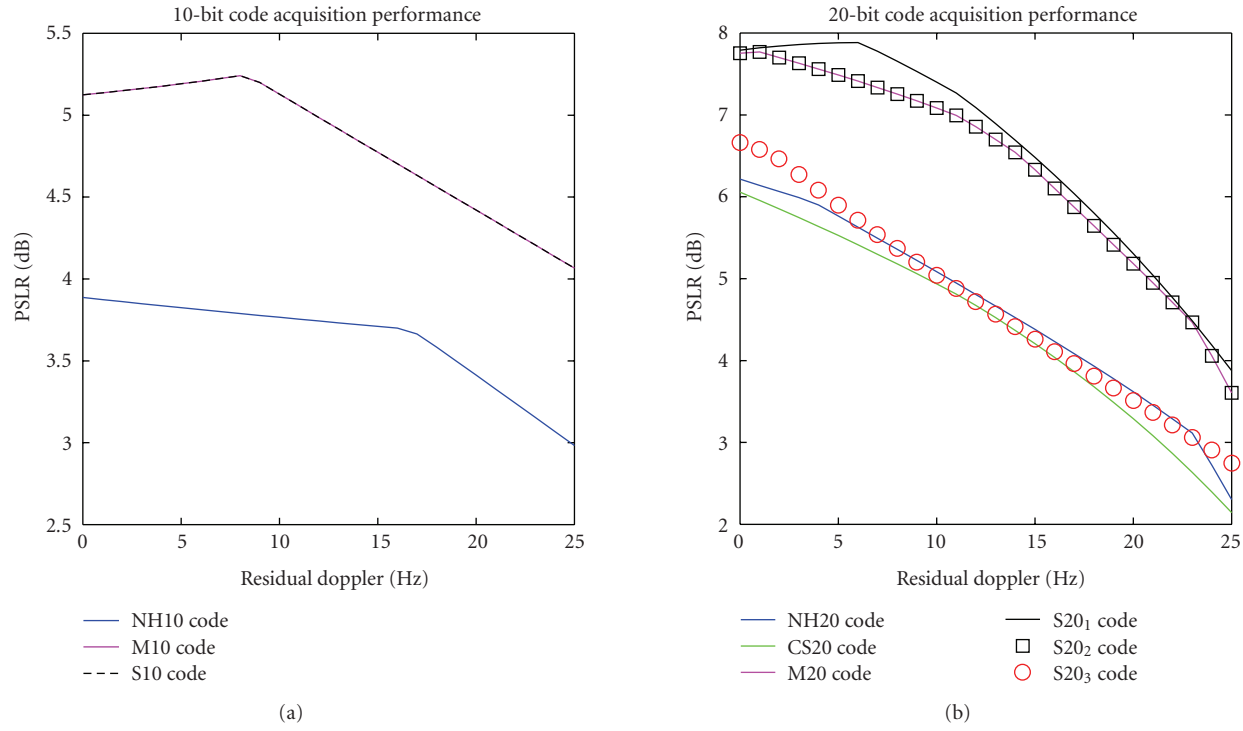

Figure 6: Effect of residual Doppler on secondary code acquisition (LHS) 10-bit code (RHS) 20-bit code.

Table 4 lists the maximum, minimum, mean, and the standard deviation of CPSLR, ISLR, and MSC measures for the Galileo CS100 and the proposed S100 codes. While the standardized CS100 code is attractive in terms of CPSLR, the proposed S100 codes were appealing in the view point of ISLR. The MSC performance of both the codes was similar. The distribution of the CPSLR and ISLR measures of the CS100 and S100 codes is plotted in Figure 4 for better

Table 6: Hexadecimal representation of proposed S100 codes.

Hexadecimal values of S100 codes Code length = 100, no. of hex. symbols = 25, no. of zero padding = 0		
C7F526E3FA9371FD49A7015B2	CE054963FA9373815247015B2	CE05497E8B4E738152405D2C6
CE05494E5A2FF381524C69740	CE05497E39537381524071AB2	CE05496180DAB38152479FC95
CE0549549FCF3381524AD80C3	CE05497DD1CA738152408B8D6	9B501C63FA9366D40707015B2
9B501C7E8B4E66D407005D2C6	9B501C4E5A2FE6D4070C69740	9B501C7E395366D4070071AB2
9B501C6180DAA6D407079FC95	9B501C549FCF26D4070AD80C3	9B501C7DD1CA66D407008B8D6
C7F526E702A4B1FD49A63F56D	C7F526CDA80E31FD49AC95FC7	C7F526FE8B4E71FD49A05D2C6
C7F526CE5A2FF1FD49AC69740	C7F526FDD1CA71FD49A08B8D6	FD169CE702A4BF45A7263F56D
FD169CCDA80E3F45A72C95FC7	FD169CE3FA937F45A727015B2	FD169CFDD1CA7F45A7208B8D6
9CB45FE702A4A72D17E63F56D	9CB45FCDA80E272D17EC95FC7	9CB45FE3FA93672D17E7015B2
9CB45FFDD1CA672D17E08B8D6	FC72A6E702A4BF1CA9A63F56D	FC72A6CDA80E3F1CA9AC95FC7
C301B56702A4B0C06D463F56D	C301B54DA80E30C06D4C95FC7	A93F9E6702A4AA4FE7863F56D
A93F9E4DA80E2A4FE78C95FC7	FBA394E702A4BEE8E5263F56D	FBA394CDA80E3EE8E52C95FC7
FBA394E3FA937EE8E527015B2	FBA394FE8B4E7EE8E5205D2C6	FBA394CE5A2FFEE8E52C69740
CE0549592BF8F3815249B501C	CE054959538FF3815249AB1C0	CE05494A7177F381524D63A20
9B501C592BF8E6D40709B501C	9B501C59538FE6D40709AB1C0	9B501C4A7177E6D4070D63A20
9CB45F8E02B6672D17FC7F526	9CB45FD92BF8E72D17E9B501C	9CB45FCA7177E72D17ED63A20
FC72A6A4A81CFF1CA9B6D5F8C	FC72A68E02B67F1CA9BC7F526	C301B524A81CF0C06D56D5F8C
C301B50E02B670C06D5C7F526	A93F9E24A81CEA4FE796D5F8C	A93F9E0E02B66A4FE79C7F526
495039CA7177D2540E6D63A20	1C056CCE5A2FC7015B2C69740	1C056CFE8B4E47015B205D2C6
1C056CD9538FC7015B29AB1C0	1C056CAB6030C7015B3527F3C	1C056C9E7F2547015B386036A
1C056CCA7177C7015B2D63A20	B257F1A4A81CEC95FC76D5F8C	B257F1CE5A2FEC95FC6C69740
4DA80E1C056C936A0398FEA4D	B257F198FD5B6C95FC79C0A92	B2A71F98FD5B6CA9C7F9C0A92
94E2EF98FD5B6538BBF9C0A92	B257F1B257F1EC95FC736A038	B2A71FB257F1ECA9C7F36A038
94E2EFB257F1E538BBF36A038	4950399C056C92540E78FEA4D	1C056C9C056C87015B38FEA4D
94E2EF9C056CA538BBF8FEA4D	49503981C6AC92540E7F8E54D	1C056C81C6AC87015B3F8E54D
495039822E3592540E7F74729	1C056C822E3587015B3F74729	B257F1822E35AC95FC7F74729

comparison. In Figure 4, we see that the standard CS100 codes achieved 1 dB improvement over proposed S100 codes for 50% of the times in terms of CPSLR. On the other hand, the proposed codes showed an 0.9 dB improvement over standard CS100 codes for 50% of the times in terms of ISLR. The CPSLR degradation observed in proposed S100 codes is inherent to its construction. Alternatively, one can utilize evolutionary techniques for the multiple-objective code optimization encountered in CS100 code design [27].

In the preceding section, we inferred the existence of multiple solutions due to the code periodicity and Table 2 listed the number of codes that accomplished the optimal correlation characteristics as predicted by (10). To further arrange them, the individual codes were utilized for code acquisition and their corresponding PSLR measure was obtained in the presence of residual frequency error. For example, the PSLR of the 10-bit and the 20-bit codes in the presence of 12 Hz residual error is plotted in Figure 5. In the case of 20-bit synchronization code, the ISLR measure was relaxed to 4 dB so as to include the remaining synchronization codes. Accordingly, we evaluated the PSLR performance of all the 20-bit codes (5079 codes as listed in Table 2) obtained via exhaustive search. Figure 5 readily confirms the existence of optimal synchronization codes that are better then the standardized codes in terms of PSLR measure. However, a question may arise on the specific Doppler setting and whether that could influence the PSLR performance. Further analysis did confirm this conjecture due to the existence of codes that were superior for certain Doppler scenarios.

Thus, the average of the PSLR over a range of Doppler (namely from 0 Hz to 25 Hz) was utilized as the selection criterion for code selection. Under the new average PSLR measure, the codes that accomplished superior correlation suppression are listed in Table 5. The S10 and $S20_1$ codes achieved the overall best performance in terms of average PSLR taken over a range of Doppler's. It should be emphasized here that both these codes were balanced and thus asserting the significance of the balanced property introduced earlier. Figure 6 shows the PSLR performance of the standard, Merten's and the proposed 10-bit and 20-bit synchronization codes during two-dimensional acquisition in the absence of background noise. The residual Doppler was searched between 0 Hz and 250 Hz in steps of 25 Hz as reported in [10].

The LHS plot in Figure 6 readily affirms the limitation of standard NH10 code and the advantage of utilizing the M10 and the proposed S10 code. Later it will be shown that the

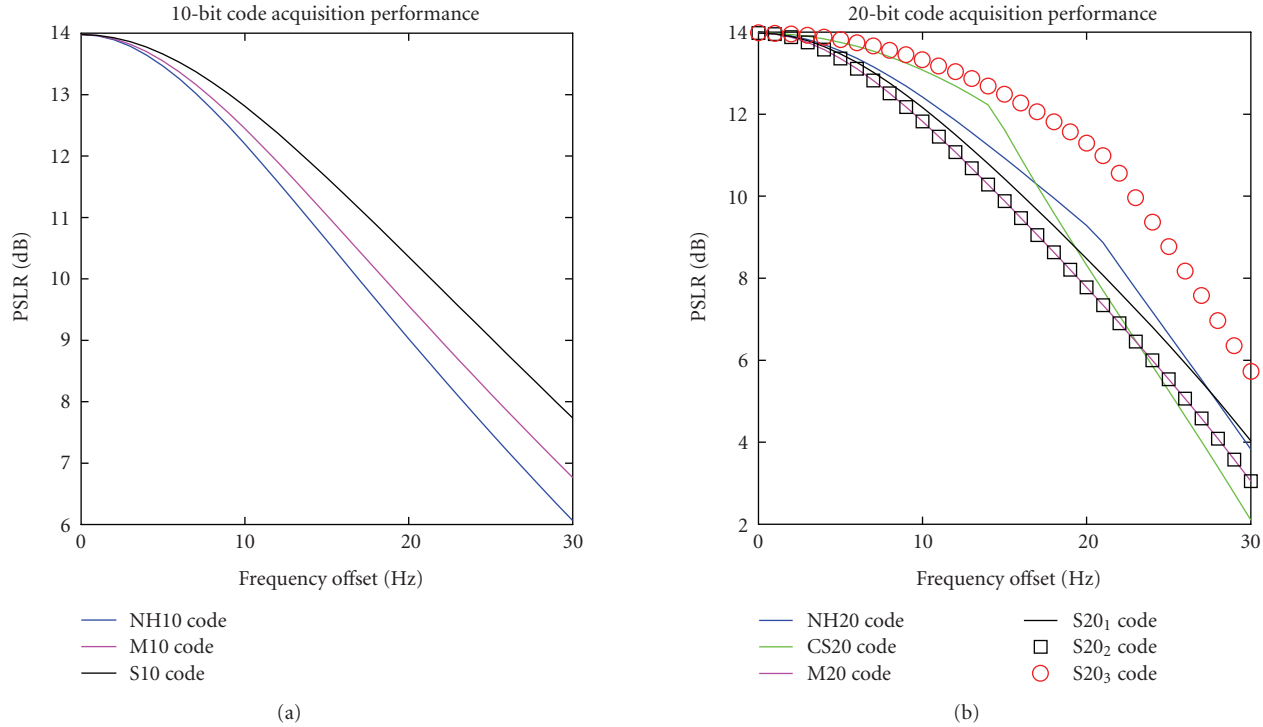

FIGURE 7: PSLR performance in the presence of frequency offset (LHS) 10-bit code (RHS) 20-bit code.

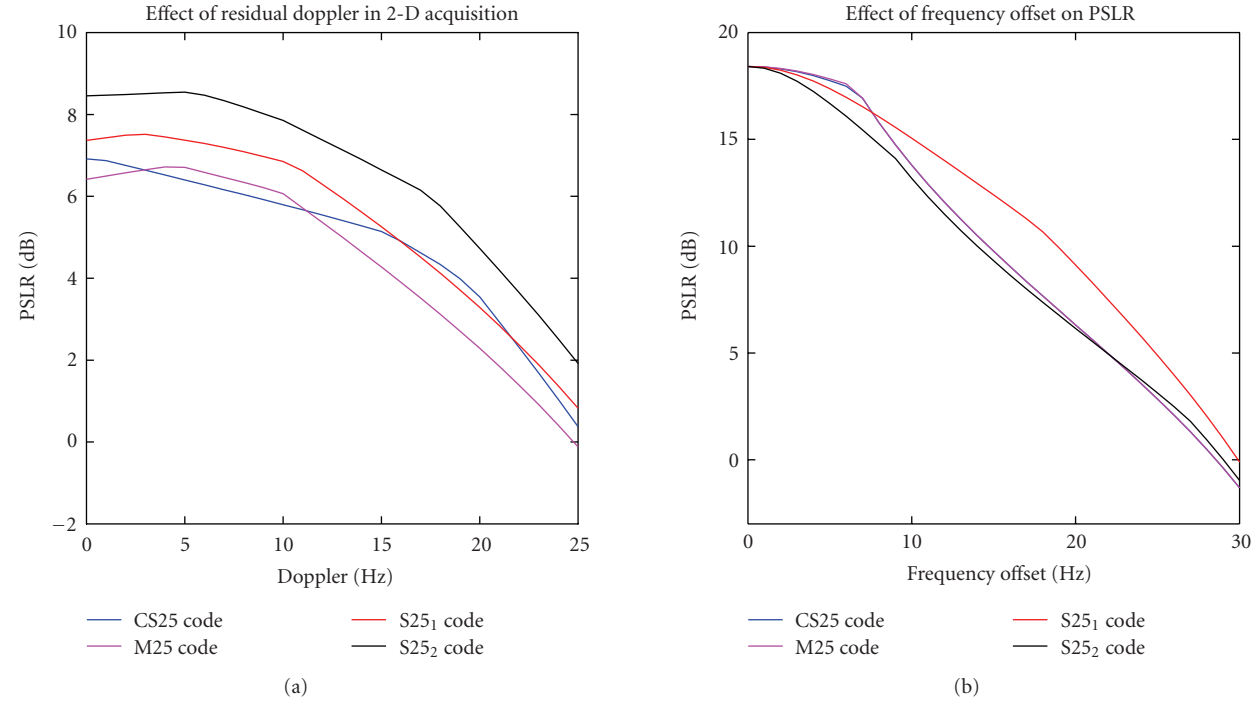

FIGURE 8: 25-bit code performance. (LHS) effect of residual Doppler on secondary code acquisition (RHS) PSLR performance as a function of frequency offset.

proposed S10 code correlation can be better than that of M10 code in the presence of frequency offset. Amongst the 20-bit codes, the Galileo CS20 code had the worst performance in accordance to result shown in Figure 5. Both the M20 code and the proposed S20$_2$ code resulted in same performance as they belong to the same equivalence class. The S20$_3$ code demonstrated similar performance as that of the NH20 code. Finally, the proposed S20$_1$ code showed the best performance

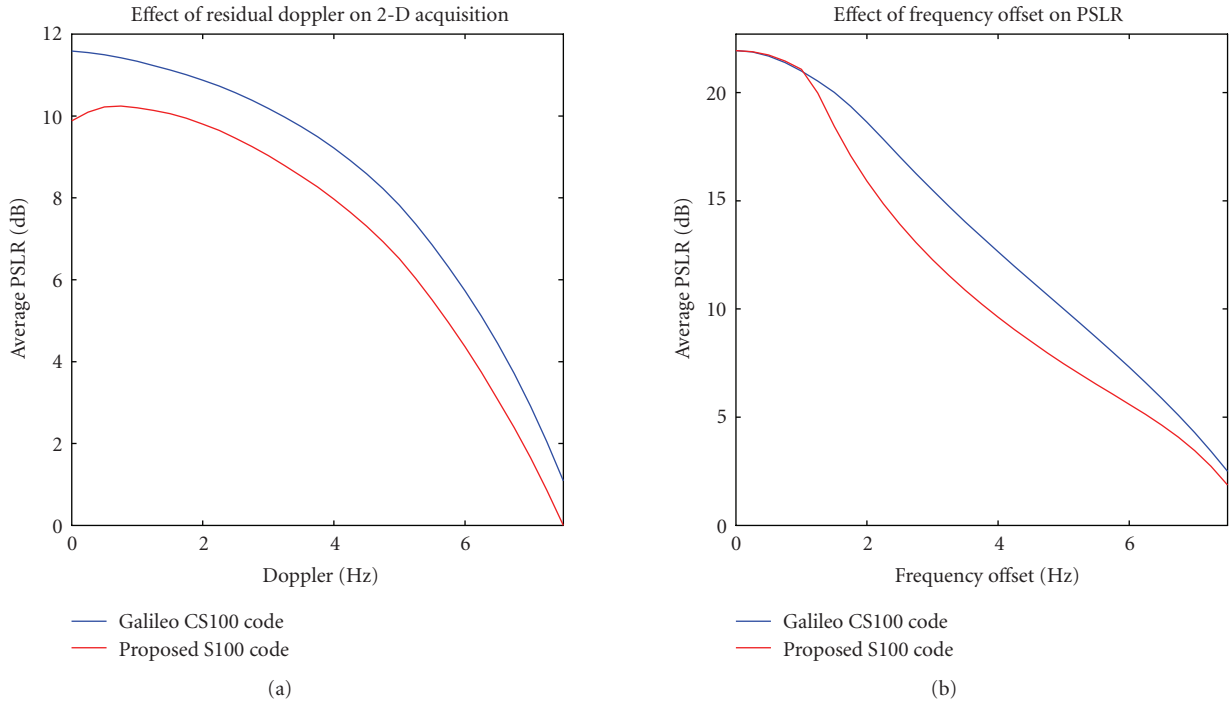

Figure 9: 100-bit code performance. (LHS) effect of residual Doppler on secondary code acquisition (RHS) PSLR performance as a function of frequency offset.

in terms of PSLR under Doppler conditions. The $S20_1$ code although suboptimal in terms of ISLR still performed better owing to its balanced property.

The correlation performance degradation in NH20 code as a function of frequency offset was analyzed in [10]. To further validate this initial observation and also to compare the correlation suppression performance of the proposed codes, numerical simulations were carried out. Figure 7 shows the PSLR performance for both 10-bit and 20-bit synchronization codes as a function of frequency offset. For the 10-bit code, one can readily notice the advantage of the proposed S10 code over the M10 and NH10 codes. In the case of 20-bit code, the standard NH20 and the CS20 codes performed better in comparison to the M20, $S20_1$, and $S20_2$ codes. On the other hand, the $S20_3$ resulted in the overall best performance and readily showed a PSLR gain of around 2.5 dB over standard NH20 and CS20 codes. However, the $S20_1$ is still attractive as it yielded the best PSLR performance as shown in Figures 6 and 7. The aforementioned analysis for a similar setting was carried out for the 25-bit code, which included the CS25, M25, and the proposed $S25_1$ and $S25_2$ codes. Note that the M25 and CS25 codes are essentially similar and are expected to perform similar. Figure 8 shows the effect of residual Doppler on secondary code acquisition and the PSLR performance as a function of frequency offset.

The standard CS25 code and that of M25 code were exactly same as far as frequency offset is concerned. However, the standard CS25 resulted in better PSLR performance as shown in LHS plot of Figure 8. On the other hand, both the proposed codes demonstrated superior PSLR performance. Interestingly, the codes $S25_1$ and $S25_2$ were complementary in their PSLR performance as shown in Figure 8. However, the code $S25_2$ can be considered optimal for not only achieving better PSLR performance (around 2 dB) in the presence of residual Doppler, it also retained similar PSLR performance to that of standard CS25 code for a wide range of frequency offsets.

Finally, the code acquisition performance of the standard CS100 and the proposed S100 codes was also evaluated in a similar manner. The residual Doppler range was reduced to 7.5 Hz so as to reflect the longer coherent integration utilized in acquiring these codes. Figure 9 shows the average PSLR performance of the standard and the proposed codes. The standard CS100 code demonstrated better performance in regards to the proposed S100 codes under both settings. The proposed code despite being characterized by better ISLR measure was still limited by its construction method from code of short length. Nevertheless, it readily corroborates the use of alternative solutions for the multiple code design problem.

6. CONCLUSIONS

The design of secondary synchronization code for GNSS system is important due to its role in acquisition and tracking. A limitation arising due to the usage of short secondary code is the apparent degradation in correlation isolation especially in the presence of residual frequency errors. This paper introduced the various performance measures that can be utilized for secondary synchronization code

optimization. Consequently, these performance measures were utilized to obtain optimal codes of various lengths via exhaustive search. This paper also established the association between the optimal codes and the systematic codes such as Golay complementary codes. The proposed secondary synchronization codes of lengths 10, 20, and 25 obtained in this fashion readily demonstrated superior correlation isolation performance in the presence of residual frequency errors. The developed S100 codes although appealing in terms of ISLR measure demonstrated inferior acquisition performance over standardized CS100 codes. Truncation of LFSR codes or code design using genetic algorithms can produce code sets with better correlation characteristics. The significance of the correlation isolation improvement demonstrated by the new synchronization codes in terms of probability of false alarm and detection is currently being investigated. Finally, judicious design of short synchronization codes can offer optimal correlation suppression and efficient signal generation.

Example 1. The NH10 Code represented by the hexadecimal value "F28" is obtained as follows:

$$\begin{aligned} \mathrm{F} &\longrightarrow 1\ 1\ 1\ 1, \\ 2 &\longrightarrow 0\ 0\ 1\ 0, \\ 8 &\longrightarrow 1\ 0\ 0\ 0. \end{aligned} \tag{17}$$

Hence, "F28" $\longrightarrow$ $1, 1, 1, 1, 0, 0, 1, 0, 1, 0, \mathbf{0}, \mathbf{0}$. The last two digits highlighted in bold are discarded, and the zero symbols are mapped in to -1. (i.e., $0 \rightarrow -1$).

REFERENCES

[1] G. W. Hein, J. Godet, J. L. Issler, et al., "Status of Galileo frequency and signal design," in *Proceedings of the 15th International Technical Meeting of the Satellite Division of the Institute of Navigation (ION GPS '02)*, pp. 266–277, Portland, Ore, USA, September 2002.

[2] T. Grelier, J. Dantepal, A. Delatour, A. Ghion, and L. Ries, "Initial observations and analysis of compass MEO satellite signals," *Inside GNSS*, pp. 39–43, June 2007.

[3] R. D. Fontana, W. Cheung, and T. Stansell, "The modernized L2 civil signal," *GPS World*, pp. 28–34, September 2001.

[4] A. J. van Dierendonck and C. Hegarty, "The new L5 civil GPS signal," *GPS World*, vol. 11, no. 9, pp. 64–71, 2000.

[5] B. C. Barker, K. A. Rehborn, J. W. Betz, et al., "Overview of the GPS M code signal," in *Proceedings of the National Technical Meeting of the Institute of Navigation (ION NTM '00)*, pp. 542–549, Anaheim, Calif, USA, January 2000.

[6] S. Pullen and P. Enge, "A civil user perspective on near-term and long-term GPS modernization," in *Proceedings of the GPS/GNSS Symposium*, p. 11, Tokyo, Japan, November 2004.

[7] Galileo SIS ICD, "Galileo Open Service: Signal In Space Interface Control Document," August 2006.

[8] J. J. Rushanan, "The spreading and overlay codes for the L1C signal," in *Proceedings of the National Technical Meeting of the Institute of Navigation (ION NTM '07)*, pp. 539–547, San Diego, Calif, USA, January 2007.

[9] L. Ries, C. Macabiau, Q. Nouvel, et al., "A software receiver for GPS-IIF L5 signal," in *Proceedings of the International Technical Meeting of the Satellite Division of the Institute of Navigation (ION GPS '02)*, pp. 1540–1553, Portland, Ore, USA, September 2002.

[10] C. Macabiau, L. Ries, F. Bastide, and J.-L. Issler, "GPS L5 receiver implementation Issues," in *Proceedings of the International Technical Meeting of the Institute of Navigation (ION GPS '03)*, pp. 153–164, Portland, Ore, USA, September 2003.

[11] S. Mertens, "Exhaustive search for low-autocorrelation binary sequences," *Journal of Physics A*, vol. 29, no. 18, pp. L473–L481, 1996.

[12] F. Soualle, M. Soellner, S. Wallner, et al., "Spreading code selection criteria for the future GNSS Galileo," in *Proceedings of the European Navigation Conference (ENC GNSS '05)*, p. 10, Munich, Germany, July 2005.

[13] C. Tellambura, M. G. Parker, Y. J. Guo, S. J. Shepherd, and S. K. Barton, "Optimal sequences for channel estimation using discrete Fourier transform techniques," *IEEE Transactions on Communications*, vol. 47, no. 2, pp. 230–238, 1999.

[14] D. V. Sarwate and M. B. Pursley, "Crosscorrelation properties of pseudorandom and related sequences," *Proceedings of the IEEE*, vol. 68, no. 5, pp. 593–619, 1980.

[15] M. Golay, "The merit factor of long low autocorrelation binary sequences (Corresp.)," *IEEE Transactions on Information Theory*, vol. 28, no. 3, pp. 543–549, 1982.

[16] M. Rupf and J. L. Massey, "Optimum sequence multisets for synchronous code-division multiple-access channels," *IEEE Transactions on Information Theory*, vol. 40, no. 4, pp. 1261–1266, 1994.

[17] A. Lempel, M. Cohn, and W. L. Eastman, "A class of balanced binary sequences with optimal autocorrelation properties," *IEEE Transactions on Information Theory*, vol. 23, no. 1, pp. 38–42, 1977.

[18] D. Jungnickel and A. Pott, "Perfect and almost perfect sequences," *Discrete Applied Mathematics*, vol. 95, no. 1–3, pp. 331–359, 1999.

[19] F. Neuman and L. Hofman, "New pulse sequences with desirable correlation properties," in *Proceedings of the IEEE National Telemetry Conference (NTC '71)*, pp. 272–282, Washington, DC, USA, April 1971.

[20] M. Golay, "Complementary series," *IEEE Transactions on Information Theory*, vol. 7, no. 2, pp. 82–87, 1961.

[21] H. Urkowitz, "Complementary-sequence pulse radar with matched filtering following doppler filtering," US patent 5151702, September 1992.

[22] H. Minn, V. K. Bhargava, and K. B. Letaief, "A robust timing and frequency synchronization for OFDM systems," *IEEE Transactions on Wireless Communications*, vol. 2, no. 4, pp. 822–839, 2003.

[23] V. Diaz, J. Urena, M. Mazo, J. J. Garcia, E. Bueno, and A. Hernandez, "Using Golay complementary sequences for multi-mode ultrasonicoperation," in *Proceedings of the 7th IEEE International Conference on Emerging Technologies and Factory Automation (ETFA '99)*, vol. 1, pp. 599–604, Barcelona, Spain, October 1999.

[24] S. Z. Budisin, "Efficient pulse compressor for Golay complementary sequences," *Electronics Letters*, vol. 27, no. 3, pp. 219–220, 1991.

[25] European Space Agency, "Galileo Open Service: Signal In Space Interface Control Document," Interface control document, European Union, May 2006, http://www.galileoic.org/la/files/Galileo%20OS%20SIS%20ICD%20230506.pdf.

[26] M. Tran and C. Hegarty, "Receiver algorithms for the new civil GPS signals," in *Proceedings of the National Technical Meeting of the Institute of Navigation (ION NTM '02)*, pp. 778–789, San Diego, Calif, USA, January 2002.

[27] S. K. Shanmugam and H. Leung, "Chaotic binary sequences for efficient wireless multipath channel estimation," in *Proceedings of the 60th IEEE Vehicular Technology Conference (VTC '04)*, vol. 60, pp. 1202–1205, Los Angeles, Calif, USA, September 2004.